Journal of Power Sources 220 (2012) 373–376

Contents lists available at SciVerse ScienceDirect

Journal of Power Sources

journal homepage: www.elsevier.com/locate/jpowsour

Short communication

Scanning probe imaging of surface ion conductance in an anion exchange membrane

Qinggang He [a,*], Xiaoming Ren [b,*]

[a] Environmental Energy Technologies Division, Lawrence Berkeley National Laboratory, 1 Cyclotron Road, Berkeley, CA 94720, USA
[b] U.S. Army Research Laboratory, 2800 Powder Mill Rd., RDRL-SED-C, Adelphi, MD 20783, USA

HIGHLIGHTS

- The surface conducting property of an anion exchanged membrane (AEM) was studied.
- The surface conductance of AEM increases exponentially as a function of relative humidity (RH).
- Better current response was found on AEM at low RH as compared to proton exchange membrane (PEM).

ARTICLE INFO

Article history:
Received 19 June 2012
Received in revised form
12 July 2012
Accepted 13 July 2012
Available online 11 August 2012

Keywords:
Anion exchange membrane
Current sensing SPM
Ionic conductivity
Fuel cells

ABSTRACT

The goal of this study was to investigate surface ion conductance variation in an anion-exchange membrane (AEM) using current-sensing scanning probe microscopy. No direct correlation was found between the membrane surface topography and local ion conductance. Smaller and larger conducting areas associated with ion channels and ionic clusters were identified in images of membrane surface ion conductance. Both the size of ion channels and the density of ionic clusters tended to increase significantly at higher relative humidity (RH) conditions. The ionic conductance of the AEM was one order of magnitude lower than its proton-exchange counterpart (Nafion®) at 100% relative humidity. This decrease may be due to the rate-limiting properties of the studied AEM, such as lower mobility of anions (HCO_3^- and OH^-), smaller size of ionic channels, lower density of ionic clusters, and lower capability for water uptake as compared to Nafion® 212. Nevertheless, the ionic conductance was found to be higher on the AEM when the RH was lower than 45%. These results have direct implications for the application of the AEM in fuel cells without humidification systems.

Published by Elsevier B.V.

1. Introduction

A key component of an alkaline-electrolyte fuel cell that determines the system performance and durability is an anion exchange membrane (AEM). [1] Different types of AEMs composed of polymer backbones with hydrophobic side chains terminated with quaternary ammonium groups have been synthesized and evaluated [2–5]. Averaged bulk properties of these AEMs, including water uptake and transport [6,7], ionic transport and conductivity [6,8,9], thermal stability [10] and ion-exchange capacity [10] have been studied. However, there are very few reports on the surface properties of AEMs, which play a critical role in the electrochemical behavior of the catalyst/membrane interface [4].

In fact, the direct contact between catalyst and ionic channels in the solid membrane electrolyte is a *sine qua non* condition for good electrochemical performance of a composite electrode [11]. A fundamental understanding of the correlation between the membrane surface topography and ion-conducting channel topology is still needed. For this purpose, *in situ* scanning probe microscopy (SPM) techniques have been developed to sense and image localized conductive domains on the surface of ion-exchange membranes under potential-controlled conditions in real time [12–16].

In this paper, we present a study of the local surface ion conductance distribution in an anion exchange solid polymer membrane at various relative humidity (RH) levels using a current-sensing (CS) atomic force microscopy (AFM) technique. The results on a nanometer scale show that the surface ionic conductance and morphology depend on the value of RH strongly. A direct comparison of surface ion conductance between AEM and Nafion® membranes was carried out.

* Corresponding authors. Tel.: +1 5104865433; fax: +1 5104867303.
E-mail addresses: hqgma2008@gmail.com (Q. He), xiaoming.ren.civ@mail.mil (X. Ren).

0378-7753/$ – see front matter Published by Elsevier B.V.
http://dx.doi.org/10.1016/j.jpowsour.2012.07.039

2. Experimental

The A-006 anion exchange membrane used in this study was obtained from the Tokuyama Corporation. A Nafion® 212 membrane was purchased from DuPont and cleaned following a standard procedure [17]. A 5500 atomic force microscope from Agilent Technologies Inc. was used to probe and image the surface of the membrane. A Nanosensors PPP-NCSTPt-10 silicon tip coated with 25 nm thick layer of PtIr was employed as both the AFM probe and the cathode in the Tip/membrane/gold system. The membrane was hot pressed directly onto a metallic sample holder coated with gold, and the AFM tip sensed the surface of the membrane in the contact mode at a tip-sample force of ~30–50 nN. A constant DC bias of 1.5 V was applied between the AFM tip and the membrane sample holder during the measurements. The resulting tip membrane/substrate current response was monitored using a 1 nA V^{-1} current–voltage converter.

All experiments were performed in an environmental chamber filled with air, wherein constant relative humidity was controlled *via* equilibration using saturated solutions of Sigma–Aldrich analytic-grade calcium chloride (RH 30%), potassium nitrite (RH 49%), sodium bromide (RH 56%), sodium nitrite (RH 65%), sodium nitrate (RH 77%), ammonium sulfate (RH 80%), and potassium chloride (RH 88%).

Hydrogen and oxygen evolution reactions proceeded on the cathode and the anode, respectively. In the case of AEM, with a positive bias hydroxide ions formed concurrently with the evolution of hydrogen were transported upward to the tip and served as the carriers of negative charge. Raster scanning was carried out on the membrane surface, and both topography and current-sensing images were recorded simultaneously.

The bulk ionic conductivity of the Nafion® 212 membrane and the Tokuyama AEM A-006 sample was measured at 30 °C at different RH values with an in-plane four-probe technique established in our previous work [16].

3. Results and discussion

Fig. 1 depicts the morphology (a–d), current-sensing images (e–h), and the distribution of surface current (i–j) of the Tokuyama AEM over a relative humidity range from 30% to 88%. Generally, the AEM is characterized by a very inhomogeneous surface topography. The weighted average height, listed in Table 1, increases with an increase in RH, indicating that the AEM sample swelled as it became more hydrated. However, the 2D average roughness (R_a, the arithmetic average of the vertical distance of measured data points from the mean height) listed in Table 1 shows only a modest variation as RH increases from 30% to 88%. The surface roughness values for AEM are close to that of a proton exchange membrane [18].

A comparison of the current-sensing images and the relative topography at the same RH values reveal that the variation of current amplitude does not follow that for the topography. This result clearly suggests that the surface conductance variation is primarily correlated with ionic conducting channels and clusters distribution rather than the variation of surface morphology. It has been shown that the capacitive current due to charging of AFM tips is too small to be detected, and only current signals associated with electrochemical reactions can be measured [14,19]. In addition, the electrochemical reactions cannot proceed unless the AFM tip is in contact with ionic networks wherein there is ion transport. Consequently, the current-sensing images reflect the distribution of ionic networks and clusters on the surface of the AEM. Fig. 1e presents a current-sensing image of the AEM at dry conditions. The AEM surface is characterized by large non-conductive domains, indicating that the OH^- transport across the membrane is greatly

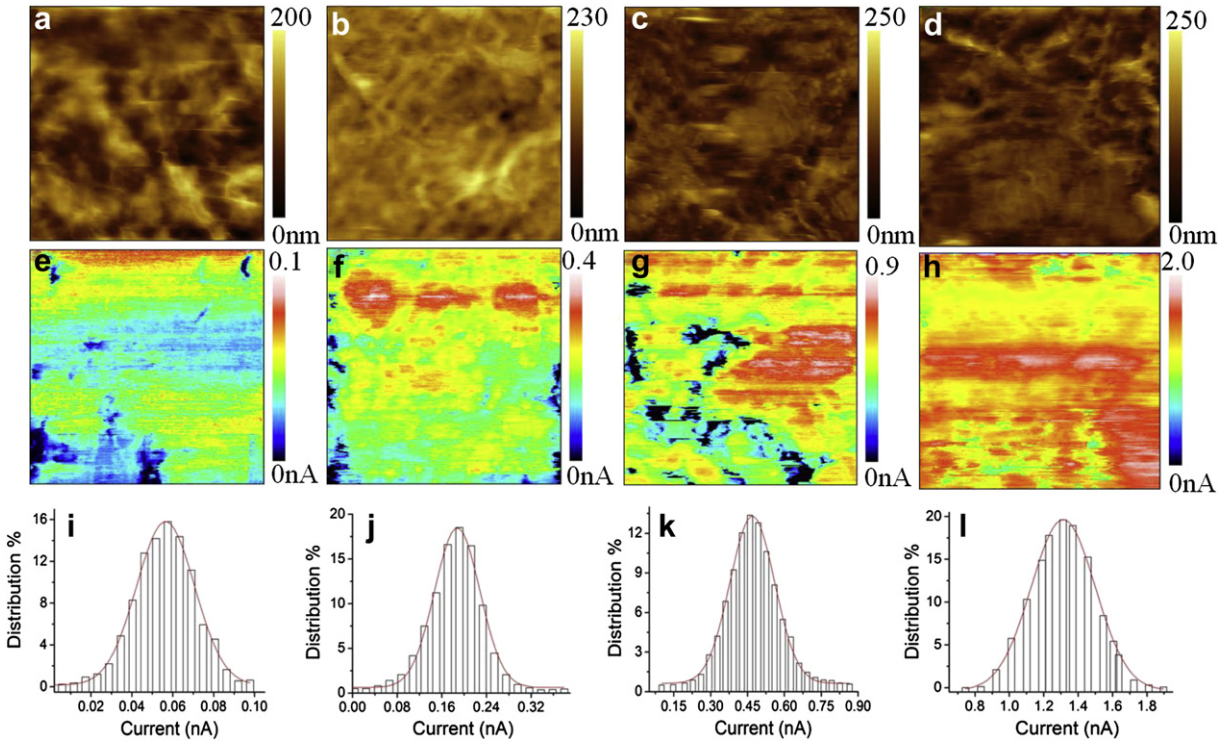

Fig. 1. Synchronized AFM topography, current-sensing image, and current distribution of Tokuyama A-006 membrane (bias voltage: 1.5 V, scan size: 5 × 5 μm^2, scan rate: 2 Hz) (a, e, i): RH = 30%; (b, f, j): RH = 53%; (c, g, k) RH = 70%; (d, h, l) RH = 88%. The red curves in the current-distribution plots indicate the Gaussian fit. (For interpretation of the references to color in this figure legend, the reader is referred to the web version of this article.)

Table 1
Current-sensing AFM results for a Tokuyama A-006 anion-exchange membrane at various values of relative humidity.

RH	30%	53%	70%	88%
H_{wa} (nm)	109.2	123.1	135.0	151.7
R_a (nm)	5.34	4.47	5.85	4.78
σ (pA)	3.6	7.9	12.5	19.1
λ	22	30	38	69
I_{wa} (nA)	0.056	0.185	0.497	1.287

H_{wa} & I_{wa}: weighted averages of the height distribution and current distribution derived from topography and current-sensing images of a Tokuyama AE-006 anion-exchange membrane.

inhibited without sufficient mobile water content. As the RH increases, more regions of the AEM surface become electrochemically active and more OH^- ions are accessible to the AFM tips, resulting in a significant enhancement of current as shown in Fig. 1f and g. However, there remains the presence of non-conducting spots (in dark blue), which are associated with the hydrophobic phase in the membrane structure. When the RH is as high as 88%, the membrane surface (Fig. 1h) is dominated by large conducting areas corresponding to hydrophilic domains, which were dry and highly resistive at lower RH [15]. It thus appears that the OH^--conducting clusters tend to branch out and merge with others and form larger aggregates.

The current distributions of the AEM membrane at different RH are shown in Fig. 1i–l. Of great interest is the observation that the conductance distributions derived from the integral current of the entire area show Gaussian fits as opposed to random surface height distributions. Similar to the results obtained in our study, a Gaussian current distribution was also observed for both Nafion® 112 and Nafion® 117 proton-exchange membranes [13]. The conduction distribution may provide information about inner ionic channels because the current flow may spread largely inside the membrane. Theoretical equations to describe the conductance distribution are shown as follows [20]:

$$C_{peak} = \lambda \cdot \sigma \quad (1)$$

$$\Delta C = 2\sqrt{2\ln 2}\sqrt{\lambda} \cdot \sigma \quad (2)$$

where C_{peak} is the center peak value; ΔC is the full width at half maximum (FWHM); σ is the current value in a single channel; and λ is the averaged number of the contacting ionic clusters with the probing tip. It has to be emphasized that the Eq. (2) is only valid when $\lambda > 10$ in order to meet the requirement that the Gaussian fitted distribution is a good approximation of a Poisson distribution.

The λ and σ values were calculated with data from Fig. 1i–l using the above equations and the results are shown in Table 1. Better conductance from a single ionic cluster that connects to anionic channels across the membrane at higher RH may result from swollen ionic channels and smaller barrier energy for OH^- ion transport. As can be expected, a larger number density of ionic clusters and membrane-spanning aqueous domains at higher RH is also observed. This result supports other researchers' claims that anion transport pathway is shorten at higher water contents for an AEM [21].

Although detailed numerical simulations, molecular-modeling methods, and other experimental techniques are required to fully unravel the origins of conductance variation with water content in AEMs, we can invoke the postulate that this variation is related to a change in the microstructure of the membrane material, based on the above CSAFM images and the calculation for λ and σ values. For a modest extent of swelling, narrow channels exist between ionic clusters, which enhance the energy barrier for ion transfer between two adjoining sides. In contrast, for great extent of swelling where all sites being considered as energetically equivalent, the anion diffusion-migration transport process is more facile.

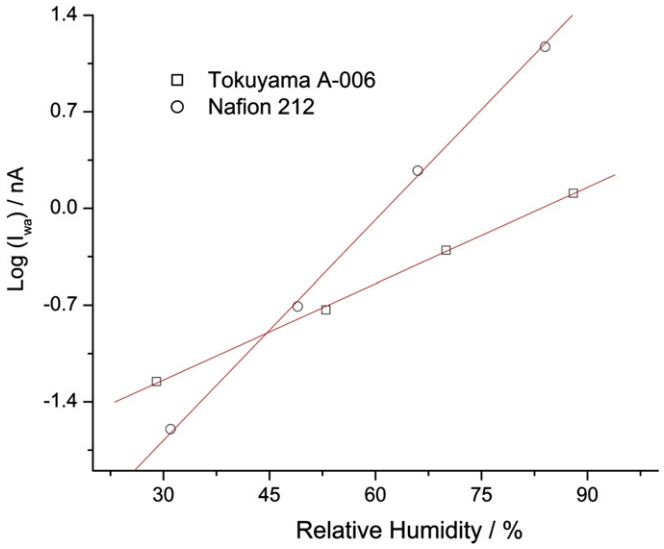

Fig. 2. Weighted averages of conduction current from current-sensing images for a Tokuyama A-006 AEM and a Nafion® 212 PEM at different relative humidity values.

With the prerequisite that the AEM and its counterpart (Nafion) were examined under exactly the same conditions, a comparison of conducting ability between these two types of membrane can be made. Fig. 2 shows logarithmic plots of weighted-average current values (I_{wa}) of current distribution *versus* RH for the AEM sample and a Nafion® 212 sample. In both cases, the log I_{wa} value increases linearly with RH. The AEM shows better conductance than Nafion® 212 at low RH (RH < 50%). Considering the fact that the Tokuyama AEM is fabricated by a radiation-graft method from polyethylene, it may have more direct conduction path than the Nafion® membrane. Nevertheless, an order of magnitude lower conductance was found on the AEM sample as compared to the Nafion® 212 membrane when the membranes become fully hydrated. A similar trend was also found with the comparison of the bulk conductivity of Nafion® 212 and the AEM sample (see Fig. S1). The enhancement of surface conductance of fully hydrated Nafion® 212 over the Tokuyama AEM can be explained by (a) The AEM sample may have a smaller rate constant for the elementary ion-transfer step due to interactions between the mobile ions and the fixed sites, (b) the smaller sizes of the ionic clusters and lower number density of ionic channels for AEM, and (c) the higher water-uptake capacity of Nafion than that of the AEM. All of these aspects play a significant role and must be taken into account when considering strategies for improvement of intrinsic properties of AEMs for applications in alkaline fuel cells.

4. Conclusion

An anion-exchange membrane (AEM, Tokuyama A-006) was studied by means of a current-sensing AFM technique. High-spatial-resolution topography and current-sensing images were recorded simultaneously. The distribution of membrane-spanning hydrophilic domains and ionic clusters, which are responsible for OH^--ion transport, were observed directly. Significantly, no correlation was observed between topographic features and the conductance distribution. Interestingly, this study also demonstrated that the conductance distribution of the AEM follows a Gaussian function at different values of RH. Based on data fitting

and calculations, we found that both the current in a single channel and the average number of clusters contacting the probing tip increase with increasing RH. We conclude that the swelling of surface and percolated ionic channels, enlarged surface contact area, and greater ion-transport rates can account for the exponential growth of surface conductance of AEM as a function of RH. Finally, reminiscent of a Nafion membrane, a linear plot of log (I_{wa}) (weighted averaged current) *versus* RH was found for the AEM. The AEM shows better current response at low RH but one order of magnitude lower I_{wa} values compared to Nafion under fully hydrated conditions.

Acknowledgment

This work was supported by the Assistant Secretary for Energy Efficiency and Renewable Energy, Office of Hydrogen, Fuel Cells and Infrastructure Technologies of the U.S. Department of Energy under Contract No. DE-AC02-05CH11231. We also thank Dr. Frank Mclarnon and Mr. Kyle Clark for helpful comments and suggestions during preparation of this manuscript.

Appendix A. Supplementary data

Supplementary data related to this article can be found online at http://dx.doi.org/10.1016/j.jpowsour.2012.07.039.

References

[1] J.R. Varcoe, R.C.T. Slade, Electrochem. Commun. 8 (2006) 839–843.
[2] M. Guo, J. Fang, H. Xu, W. Li, X. Lu, C. Lan, K. Li, J. Memb. Sci. 362 (2010) 97–104.
[3] M.R. Hibbs, C.H. Fujimoto, C.J. Cornelius, Macromolecules (Washington, DC, U.S.) 42 (2009) 8316–8321.
[4] V.V. Shevchenko, M.A. Gumennaya, Theor. Exp. Chem. 46 (2010) 139–152.
[5] Y. Xiong, Q.L. Liu, Q.G. Zhang, A.M. Zhu, J. Power Sourc. 183 (2008) 447–453.
[6] M.R. Hibbs, M.A. Hickner, T.M. Alam, S.K. McIntyre, C.H. Fujimoto, C.J. Cornelius, Chem. Mater. 20 (2008) 2566–2573.
[7] T. Yamanaka, T. Takeguchi, H. Takahashi, W. Ueda, J. Electrochem. Soc. 156 (2009) B831–B835.
[8] D. Xie, G. Wang, Y. Weng, D. Chu, R. Chen, ECS Trans. 25 (2010) 3–14.
[9] L. Franck-Lacaze, P. Huguet, P. Sistat, Desalination 200 (2006) 155–156.
[10] H. Yanagi, K. Fukuta, ECS Trans. 16 (2008) 257–262.
[11] R. O'Hayre, Probing Electrochemistry at the Micro Scale: Applications in Fuel Cells, Ionics, and Catalysis, VDM Verlag Dr. Müller, 2008.
[12] F.-R.F. Fan, A.J. Bard, Sci. (Washington, D. C.) 270 (1995) 1849–1851.
[13] X. Xie, O. Kwon, D.-M. Zhu, T. Van Nguyen, G. Lin, J. Phys. Chem. B. 111 (2007) 6134–6140.
[14] R. Hiesgen, E. Aleksandrova, G. Meichsner, I. Wehl, E. Roduner, K.A. Friedrich, Electrochim. Acta. 55 (2009) 423–429.
[15] D.A. Bussian, J.R. O'Dea, H. Metiu, S.K. Buratto, Nano Lett. 7 (2007) 227–232.
[16] Q. He, A. Kusoglu, T. Lucas Ivan, K. Clark, Z. Weber Adam, R. Kostecki, J. Phys. Chem. B. 115 (2011) 11650–11657.
[17] D. Weng, J.S. Wainright, U. Landau, R.F. Savinell, J. Electrochem. Soc. 143 (1996) 1260–1263.
[18] S. Hink, E. Aleksandrova, E. Roduner, ECS Trans. 33 (2010) 57–70.
[19] E. Aleksandrova, R. Hiesgen, D. Eberhard, K.A. Friedrich, T. Kaz, E. Roduner, Chem. Phys. Chem. 8 (2007) 519–522.
[20] Y. Kang, O. Kwon, X. Xie, D.-M. Zhu, J. Phys. Chem. B. 113 (2009) 15040–15046.
[21] H. Xu, J. Fang, M. Guo, X. Lu, X. Wei, S. Tu, J. Memb. Sci. 354 (2010) 206–211.